A. S. FOUDA, G. Y. ELEWADY,
A. EL-ASKALANY, K. SHALABI

Scientific paper
UDC:620.197.3:669.717

Inhibition of aluminum corrosion in hydrochloric acid media by three Schiff base compounds

The corrosion behavior of aluminum in 0.5 M HCl solution in the absence and presence of (E)-3,6-dibromo-2-((4-methoxyphenylimino)methyl)phenol(I),(E)-3,6-dibromo-2-((4-chlorophenylimino) methyl) phenol (II) and (E)-4-(3,6-dibromo-2-hydroxybenzylideneamino)benzoic acid(III)was investigated using potentiodynamic polarization, electrochemical impedance spectroscopy (EIS) and electrochemical frequency modulation (EFM) techniques. The inhibitive action of the investigated compounds was discussed in terms of blocking the electrode surface by adsorption of the molecules through the active centers contained in their structures. The adsorption of these derivatives on aluminum surface is consistent with Freundlich adsorption isotherm. The effect of temperature on the rate of corrosion in the absence and presence of these compounds were also studied. Physical adsorption mechanism is proposed from the calculated thermodynamic parameters for all investigated compounds. Quantum chemical parameters such as the highest occupied molecular orbital energy (E_{HOMO}), the lowest unoccupied molecular orbital energy (E_{LUMO}), energy gap (ΔE), dipole moment (μ), electronegativity (χ), chemical potential (P_i), global hardness (η) and softness (σ), were calculated. Quantum chemical studies indicate that the inhibition potentials of these compounds correlate well with $E_{HOMO,}$ $\Delta E, \eta$, σ, P_i, $\chi$and ΔN. A good correlation was found between the theoretical data and the experimental results.

***Key words**: Aluminum, corrosion, HCl, quantum chemical calculation, PM3, Schiff bases.*

1. INTRODUCTION

Corrosion of aluminum and its alloys has been a subject of numerous studies due to their high technological value and wide range of industrial applications especially in aerospace and house-hold industries. Aluminum and its alloys, however, are reactive materials and are prone to corrosion. A strong adherent and continuous passive oxide film is developed on Al upon expo or aqueous solutions. This surface film is amphoteric and dissolves when the metal is exposed to high concentrations of acids or bases [1]. Hydrochloric acid solutions are used for pickling, chemical and electrochemical etching of aluminum. It is very important to add corrosion inhibitors to prevent metal dissolution and minimize acid consumption [2]. The choice of inhibitor is based on two considerations: first it could be synthesized conveniently from relatively cheap raw materials; secondly, it contains the electron cloud on the aromatic ring or electronegative atoms such as nitrogen, oxygen in relatively long-chain compounds. Numerous organic substances containing polar functions with nitrogen, oxygen, and/or sulphur atoms and aromatic rings in a conjugated system have been reported to exhibit good inhibiting properties [3-5]. Aliphatic and aromatic amines as well as nitrogen heterocyclic compounds were used as corrosion inhibitors for Al dissolution in acidic media [6-12]. Some Schiff bases have been reported earlier as corrosion inhibitors for aluminum [13], zinc [14], iron [15] and copper [16-18]. Several Schiff bases have also been investigated as corrosion inhibitors for mild steel in acidic media [19-21].

Address author: Department of Chemistry, Faculty of Science, El-Mansoura University, El-Mansoura- 35516, Egypt

The objective of the present investigation is to study the corrosion inhibition activity of the investigated Schiff bases by potentiodynamic polarization, ac impedance spectroscopy and electrochemical frequency modulation and quantum chemical calculations. Also, to explore correlations between advanced quantum chemical concepts and inhibition efficiency.

2. EXPERIMENTAL

Al metal was provided from ‘‘Aluminum Company of Egypt, Nagh Ammady’’ ,its chemical composition is 0.100%Si, 0.250% Fe, 0.047% Mn, 0.007% Mg, 0.002% Ni, 0.008% Cr, 0.003% Zn, 0.012% Ga, 0.001% Na, 0.007% V, 0.001% Zr, 0.007% Ti and 99.550% Al.

Electrochemical experiments were performed using a typical three-compartment glass cell consisted of the aluminum specimen as working electrode, saturated calomel electrode (SCE) as a reference electrode and a platinum foil (1.0 cm^2) as a counter electrode. The reference electrode was connected to a Luggin capillary and the tip of the Luggin capillary is made very close to the surface of the working electrode to minimize IR drop. The cell was open to air and the measurement was conducted at room temperature. All potential values were reported versus SCE. Prior to every experiment, the electrode was abraded with successive different grades of emery paper, degreased with alkaline solution [22] and washed with bidistilled water and finally dried.

Tafel polarization curves were obtained by changing the electrode potential automatically from (-800 to 500 mV_{SCE}) at open circuit potential with a scan rate of 5 mVs^{-1}. Stern-Geary method [23] used for the determination of corrosion current is performed by extrapolation of anodic and cathodic Tafel lines of charge transfer controlled corrosion reactions to a point which

gives log I_{corr} and the corresponding corrosion potential (E_{corr}) for inhibitor free acid and for each concentration of inhibitor. Then I_{corr} was used for calculation of inhibition efficiency and surface coverage (θ) as below:

$$\%IE = (1- [i_{corr(inh)} / i_{corr(free)}]) \times 100 \quad (1)$$

$$\theta = 1- [i_{corr(inh)} / i_{corr(free)}] \quad (2)$$

where $i_{corr(free)}$ and $i_{corr(inh)}$ are the corrosion current densities in the absence and presence of inhibitor, respectively.

Impedance measurements were carried out in frequency range from 10^5 Hz to 0.5 Hz with amplitude of 5 mV peak-to-peak using ac signals at open circuit potential. The experimental impedance were analyzed and interpreted on the basis of the equivalent circuit. The main parameters deduced from the analysis of Nyquist diagram are the resistance of charge transfer R_{ct} (diameter of high frequency loop) and the capacity of double layer C_{dl} which is defined as:

$$C_{dl} = 1/ (2 \pi f_{max} \ R_{ct}) \quad (3)$$

The inhibition efficiencies and the surface coverage (θ) obtained from the impedance measurements are defined by the following relations:

$$\%IE = (1- [R°_{ct}/R_{ct}]) \times 100 \quad (4)$$

$$\theta = 1-[R°_{ct}/R_{ct}] \quad (5)$$

where R^o_{ct} and R_{ct} are the charge transfer resistance in the absence and presence of inhibitor, respectively.

Electrochemical frequency modulation, EFM, was carried out using two frequencies 2 and 5 Hz. The base frequency was 0.1 Hz, so the waveform repeats after 1 s. The higher frequency must be at least two times the lower one. The higher frequency must also be sufficiently slow that the charging of the double layer does not contribute to the current response. Often, 10 Hz is a reasonable limit. The Intermodulation spectra contain current responses assigned for harmonical and intermodulation current peaks. The larger peaks were used to calculate the corrosion current density (I_{corr}), the Tafel slopes (β_c and β_a) and the causality factors CF2& CF3 [24-25].

The electrode potential was allowed to stabilize 30 min before starting the measurements. All the experiments were conducted at 20 ± 1°C. Measurements were performed using Gamry Instrument Potentiostat/ Galvanostat/ZRA. This includes a Gamry framework system based on the ESA 400. Gamry applications include dc105 for dc corrosion measurements, EIS300 for electrochemical impedance spectroscopy and EFM 140 for electrochemical frequency modulation measurements along with a computer for collecting data. Echem Analyst 5.58 software was used for plotting, graphing, and fitting data.

The molecular structures of the investigated compounds were optimized initially with PM3 semiempirical method so as to speed up the calculations.

The calculated quantum chemical parameters χ, Pi and η were calculated. The concepts of these parameters are related to each other [26-30] where:

$$Pi = -\chi \quad (6)$$

$$Pi = (E_{HOMO} + E_{LUMO}) /2 \quad (7)$$

$$\eta = (E_{LUMO} - E_{HOMO}) /2 = \Delta E / 2 \quad (8)$$

The inverse of the global hardness is designated as the softness σ as follows:

$$\sigma = 1/\eta \quad (9)$$

The obtained values of v and g were used to calculate the fraction of electrons transferred, ΔN, from the inhibitor to metallic surface [31-33] as follows:

$$\Delta N = (\chi_{Al} - \chi_{inh}) /2 (\eta_{Al} + \eta_{inh}) \quad (10)$$

All chemicals and reagents were of analytical grade. The measurements were performed in 0.5 M HCl without and with the presence of the investigated compounds in the concentration range ($1x10^{-5}$ to$1x10^{-3}$ M).

The names and molecular structures of the investigated compounds are:

	Name	Structure	Molecular weight& Chemical formula
I	(E)-3,6-dibromo-2-((4-methoxyphenylimino) methyl)phenol	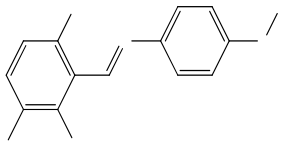	385.05 $C_{14}H_{11}Br_2NO_2$
II	(E)-3,6-dibromo-2-((4-chlorophe-nylimino)methyl) Phenol	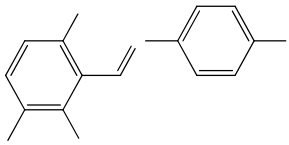	389.47 $C_{13}H_8Br_2ClNO$
III	(E)-4-(3,6-dibromo-2-hydroxy-benzylideneamino) benzoic acid	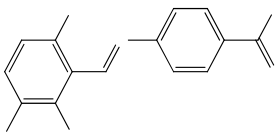	399.03 $C_{14}H_9Br_2NO_3$

3. RESULTS AND DISCUSSION

3.1-Tafel polarization study

The potentiodynamic polarization curves for Al in 0.5 M HCl solutions containing different concentrations of compound (I) at 20°C are shown in Fig. 1. Similar curves were obtained for other compounds (not shown). The intersection of Tafel regions of cathodic and anodic branches gives the corrosion current density (i_{corr}) and the corrosion potential (E_{corr}). Table 1 shows the electrochemical parameters (corrosion potential, E_{corr}, anodic and cathodic Tafel slopes, β_a, β_c, and corrosion current density, i_{corr},) obtained from Tafel plots for the Al electrode in 0.5 M HCl solution without and with different concentrations of investigated compounds.

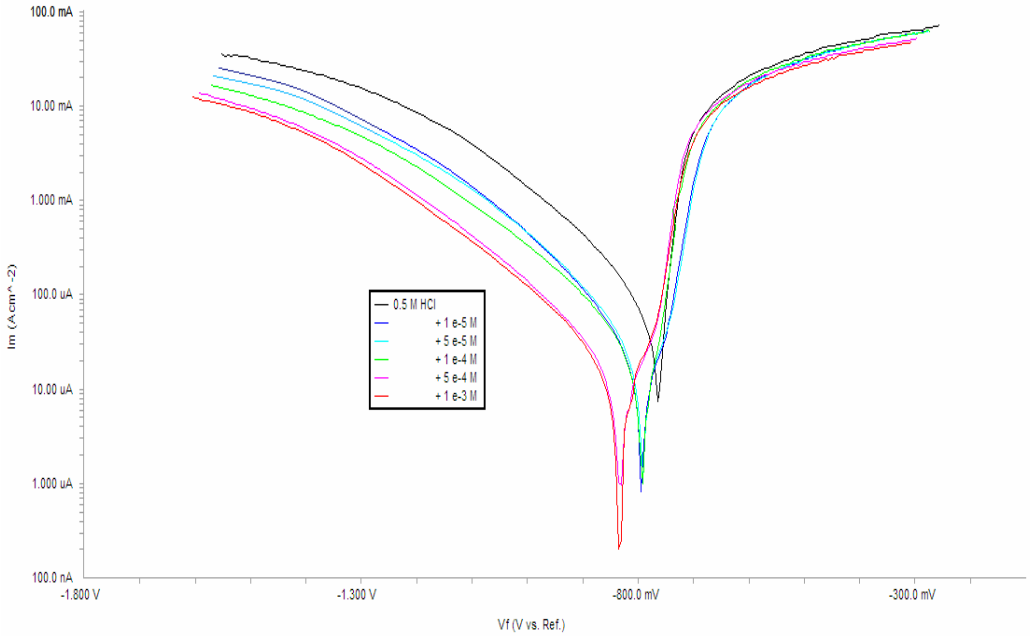

Figure (1). Potentiodynamic polarization curves for Al in 0.5 M HCl solution without and with various concentrations (10^{-5}-10^{-3} M) of compound (I) at 20 ˚C

Table 1 - The effect of concentration of the investigated compounds on the free corrosion potential (E_{corr}), corrosion current density (i_{corr}), Tafel slopes (β_a& β_c), inhibition efficiency (% IE) ,degree of surface coverage (θ) and corrosion rate for the corrosion of Al in 0.5 M HCl at 20˚C

Concentration,M		i_{corr}, µA cm^{-2}	-E_{corr}, mV vs.SCE	β_a, mV$_{SCE}$ dec^{-1}	β_c, mV$_{SCE}$ dec^{-1}	CR mpy	θ	% IE
0.5 M HCl		49.60	763	36	158	106.3	--	--
Compound I	1x10^{-5}	23.80	794	52	164	50.9	0.520	52.0
	5x10^{-5}	18.40	791	46	150	39.5	0.629	62.9
	1x10^{-4}	17.10	832	54	192	36.7	0.655	65.5
	5x10^{-4}	12.30	791	41	157	26.4	0.752	75.2
	1x10^{-3}	5.49	790	45	151	11.8	0.889	88.9
Compound II	1x10^{-5}	24.00	827	39	166	51.4	0.516	51.6
	5x10^{-5}	18.80	795	38	155	42.6	0.621	62.1
	1x10^{-4}	17.20	835	50	180	36.8	0.653	65.3
	5x10^{-4}	13.80	836	46	183	29.7	0.722	72.2
	1x10^{-3}	10.10	838	56	151	12.1	0.796	79.6
Compound III	1x10^{-5}	24.80	814	46	200	57.6	0.500	50.0
	5x10^{-5}	19.10	830	56	183	41.0	0.615	61.5
	1x10^{-4}	18.30	805	69	184	39.1	0.631	63.1
	5x10^{-4}	14.20	808	45	146	32.7	0.714	71.4
	1x10^{-3}	10.50	838	60	152	13.1	0.788	78.8

Inspection of Figure 1 shows that the addition of compound (I) has an inhibitive effect in the both anodic and cathodic parts of the polarization curves and the addition of compound (I) generally shifted the E_{corr} value towards the negative direction compared to the uninhibited Al. Thus, addition of this inhibitor reduces the Al dissolution as well as retards the hydrogen evolution reaction. In addition, parallel cathodic Tafel curves in Fig. 1 show that the hydrogen evolution is activation-controlled and the reduction mechanism is not affected by the presence of the inhibitor [34]. The anodic curves of Al in 0.5 M HCl in the presence of compound (I) show that the tested compound has no effect at potential higher than $E_{corr,}$ may be the result of significant Al dissolution leading to a desorption of the inhibiting layer. In this case, the desorption rate of the inhibitor is higher than its adsorption rate [35]. So, it could be concluded that this compound is of the mixed-type bur dominantly act as a cathodic inhibitor for Al in 0.5 M HCl medium, which may be adsorbed on the cathodic sites of the Al and reduce the evolution of hydrogen. This limitation of inhibitory action on cathodic domain is found by different researchers [36, 37]. Moreover, the adsorption of this compound on anodic sites through the lone pair of electrons of N and O atoms will then reduce the anodic dissolution of Al. The data of Table 1 revealed that I_{corr} decreases considerably with increasing the inhibitor concentration, while no definite trend was observed in the shift of E_{corr} values. The Tafel slopes show slight changes with addition of inhibitors, which suggests that the inhibiting action occurred by simple blocking of the available cathodic and anodic sites on Al surface. The dependence of % IE versus inhibitor concentration is also presented in Table 1. The obtained efficiencies indicate these investigated compounds act as effective inhibitors.

The order of decreasing inhibition efficiency of the investigated compounds was found to be: I > II > III.

3.2. Electrochemical impedance spectroscopy measurements

Electrochemical impedance spectroscopy provides a new method to characterize the film coverage on the electrode, which is related to charge transfer resistance (R_{ct}). The interface capacitance can also be used to determine the film quality [38-42]. It is known that the coverage of an organic substance on the metal surface depends not only on the structure of the organic substance and the nature of the metal, but also on the experimental conditions such as immersion time and concentration of adsorbent [41, 42]. Figure 3a shows the Nyquist plots for aluminum in 0.5 M HCl solution in the absence and presence of different concentrations of compound (I) at 20 ^{o}C. Similar curves were obtained for other two Schiff bases (not shown). All the impedance spectra were measured at the corresponding open-circuit potentials. The fact that impedance diagrams have an approximately semi-circular appearance shows that the corrosion of Al in 0.5 M HCl is controlled by a charge-transfer resistance process. Small distortion was observed in some diagrams, this distortion has been attributed to frequency dispersion [43] as a result of surface roughness, impurities, dislocations, grain boundaries, adsorption of inhibitors, formation of porous layers and in homogenates of the electrode surface. Inspections of the data reveal that each impedance diagram consists of a large capacitive loop with one capacitive time constant in the Bode –phase plots (Fig. 3b). The diameter of the capacitive loop increases with increasing concentration and were indicative of the degree of inhibition of the corrosion process. In addition to the high frequency capacitive loop, the semi-circles rolled over and extended to the fourth quadrant, and a pseudo-inductive loop at low frequency end was observed, indicating that Faradic process is taking place on the free electrode sites. This inductive loop is generally attributed to the adsorption of species resulting from the Al dissolution and the adsorption of hydrogen [44].

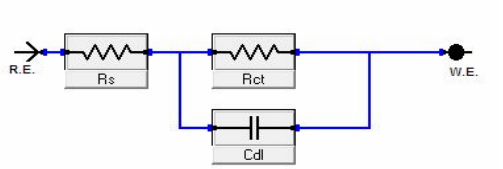

Figure 2 - Electrical equivalent circuit used to fit the impedance data

The electrical equivalent circuit model shown in Figure 2 was used to analyze the obtained impedance data. The model consists of the solution resistance (R_s), the charge-transfer resistance of the interfacial corrosion reaction (R_{ct}) and the double layer capacitance (C_{dl}). Excellent fit with this model was obtained with our experimental data.

Table 2 -Electrochemical kinetic parameters obtained by EIS technique for Al in 0.5M HCl solutions containing various concentrations of the investigated compounds at 20˚C

Concentration, M		R_{ct}, kΩ cm^2	C_{dl}, µF cm^{-2}	θ	% IE
0.5 M HCl		0.707	16.31	--	--
Compound I	1x10^{-5}	1.480	15.38	0.522	52.2
	5x10^{-5}	1.706	15.90	0.586	58.6
	1x10^{-4}	1.921	14.14	0.632	63.2
	5x10^{-4}	2.384	10.269	0.703	70.3
	1x10^{-3}	3.772	8.76	0.813	81.3
Compound II	1x10^{-5}	1.337	15.85	0.471	47.1
	5x10^{-5}	1.705	14.90	0.585	58.5
	1x10^{-4}	1.857	13.52	0.619	61.9
	5x10^{-4}	2.222	12.60	0.682	68.2
	1x10^{-3}	3.174	12.04	0.777	77.7
Compound III	1x10^{-5}	1.301	14.11	0.457	45.7
	5x10^{-5}	1.481	13.57	0.523	52.3
	1x10^{-4}	1.803	13.45	0.608	60.8
	5x10^{-4}	2.103	13.14	0.664	66.4
	1x10^{-3}	2.648	12.99	0.733	73.3

EIS data (Table 2) show that the R_{ct} values increases and the C_{dl} values decreases with increasing the inhibitor concentrations. This is due to the gradual replacement of water molecules by the adsorption of the inhibitor molecules on the metal surface, decreasing the extent of dissolution reaction. The high (R_{ct}) values, are generally associated with slower corroding system [45, 46]. The decrease in the C_{dl} can result from the decrease of the local dielectric constant and/or from the increase of thickness of the electrical double layer [47], suggested that the inhibitor molecules function by adsorption at the metal/solution interface.

The % IE obtained from EIS measurements are close to those deduced from polarization and weight loss methods. The order of inhibition efficiency obtained from EIS measurements is as follows: I > II > III.

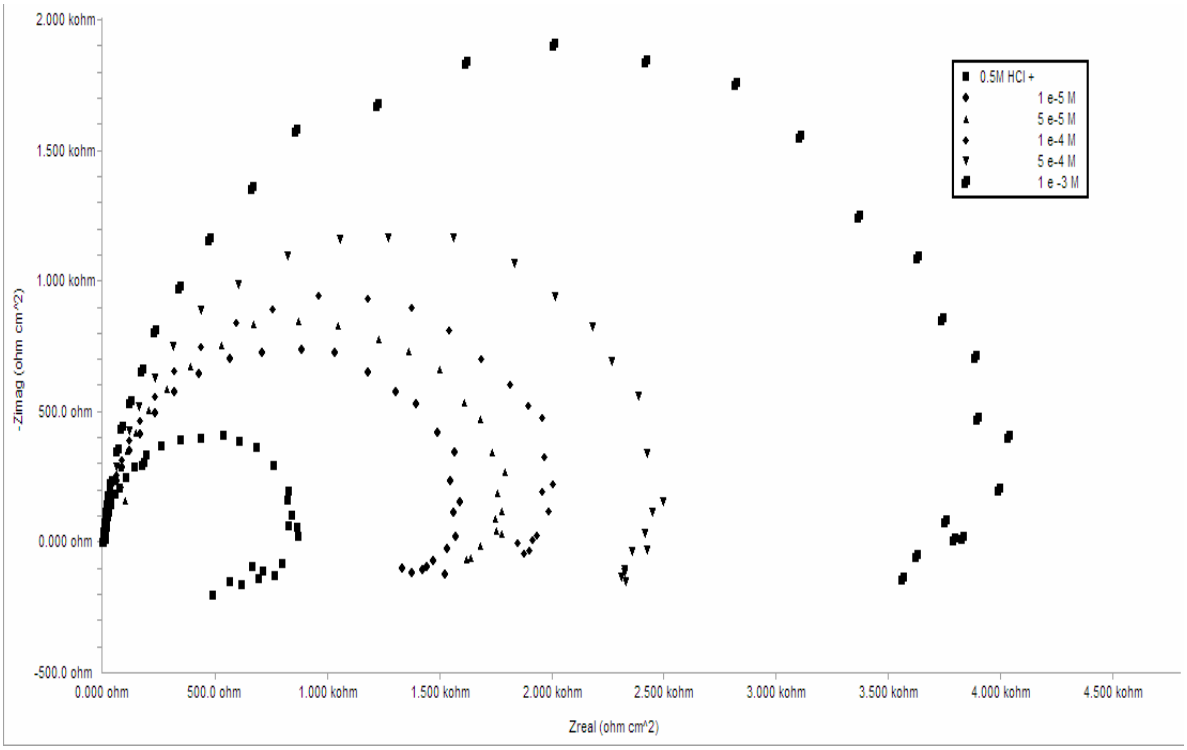

Figure 3a - Nyquist plots recorded for Al in 0.5 M HCl solutions without and with various concentrations (10^{-5}-10^{-3}M) compound I at the respective corrosion potentials and 20˚C

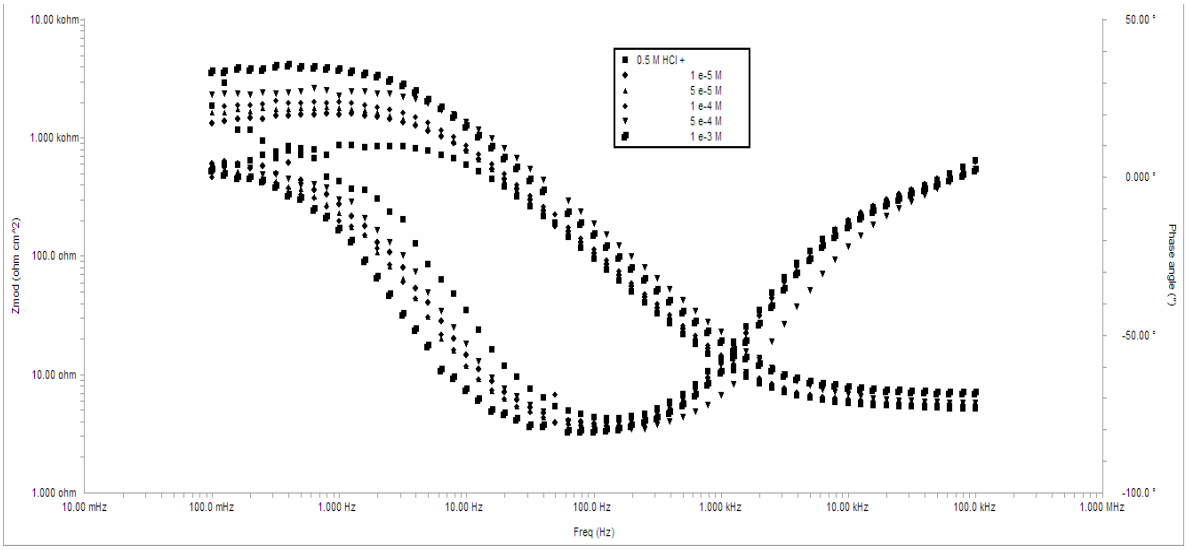

Figure 3b - Bode plots recorded for Al in 0.5M HCl solutions without and with various concentrations (10^{-5}-10^{-3}M) compound (I) at the respective corrosion potentials and 20˚C

3.3. Electrochemical frequency modulation measurements (EFM)

The EFM is a nondestructive corrosion measurement technique that can directly give values of the corrosion current without prior knowledge of Tafel constants. Like EIS, it is a small ac signal. Intermodulation spectra obtained from EFM measurements are presented in Figures 4a, 4b, 4c, 4d, 4e, 4f and 4g are examples of Al in aerated 0.5 M HCl solutions devoid of and containing different concentrations of compound (I) at 20˚C. Similar intermodulation spectra were obtained for other compounds (not shown). Each spectrum is a current response as a function of frequency. The two large peaks are the response to the 2 Hz and 5Hz excitation frequencies. These peaks are used by the EFM140 software package to calculate the corrosion current and Tafel constants.

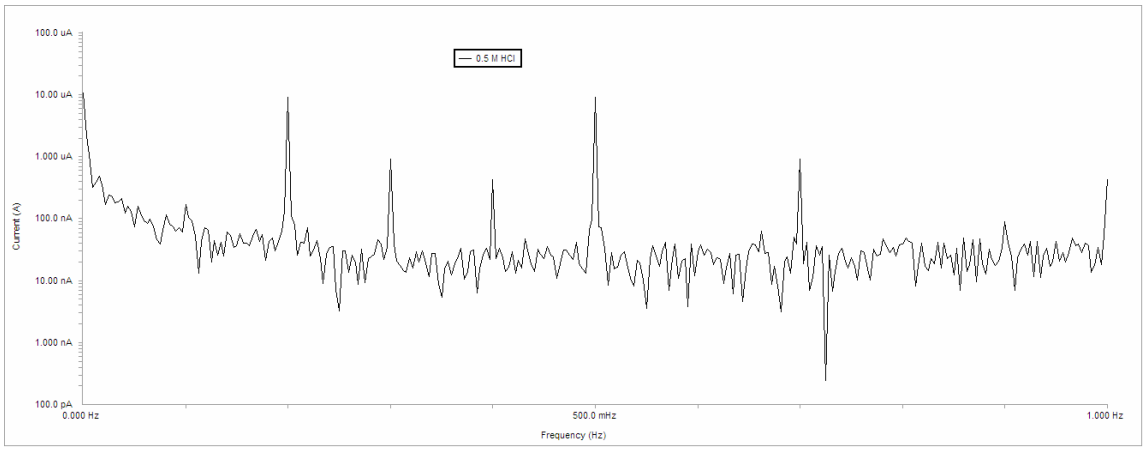

a)

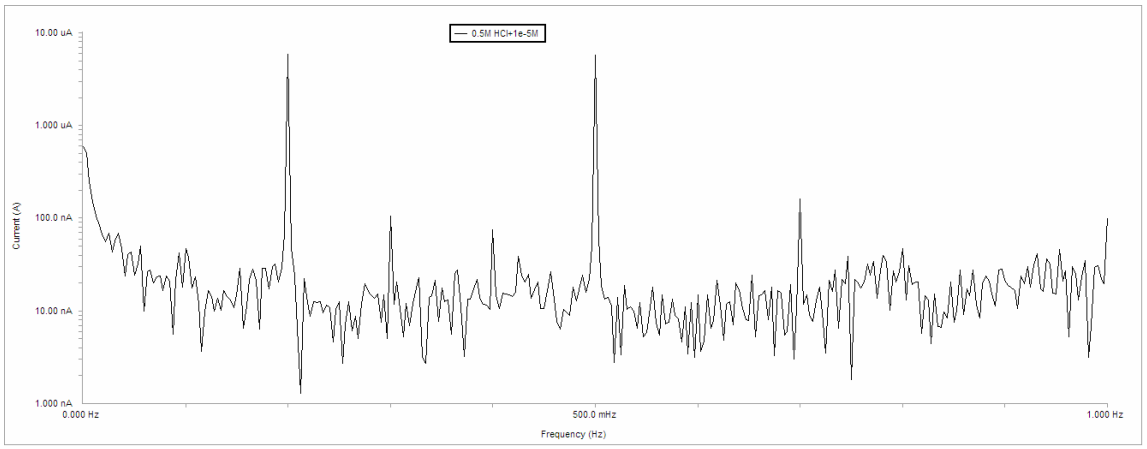

b)

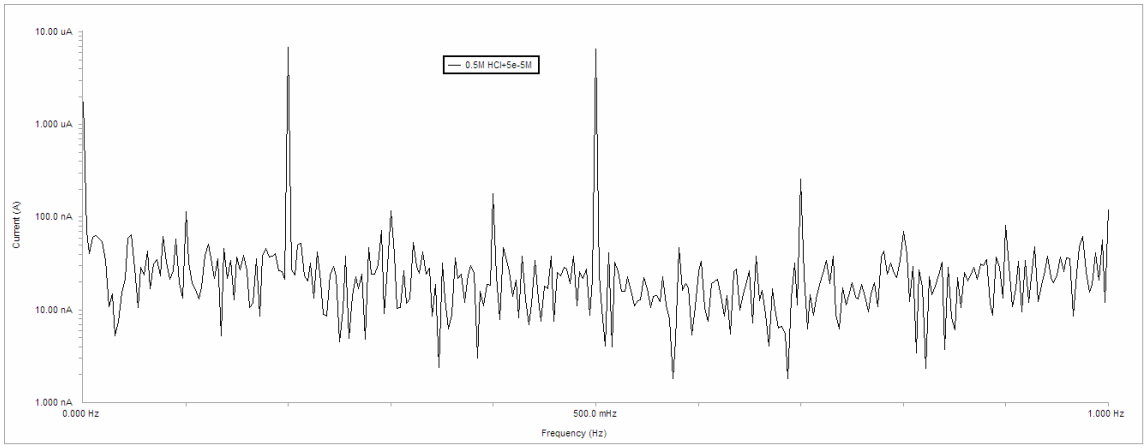

c)

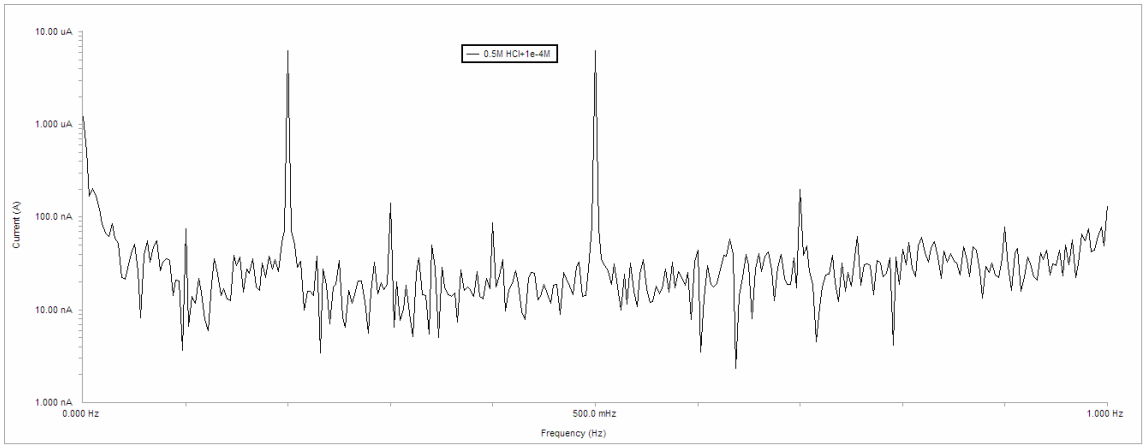

d)

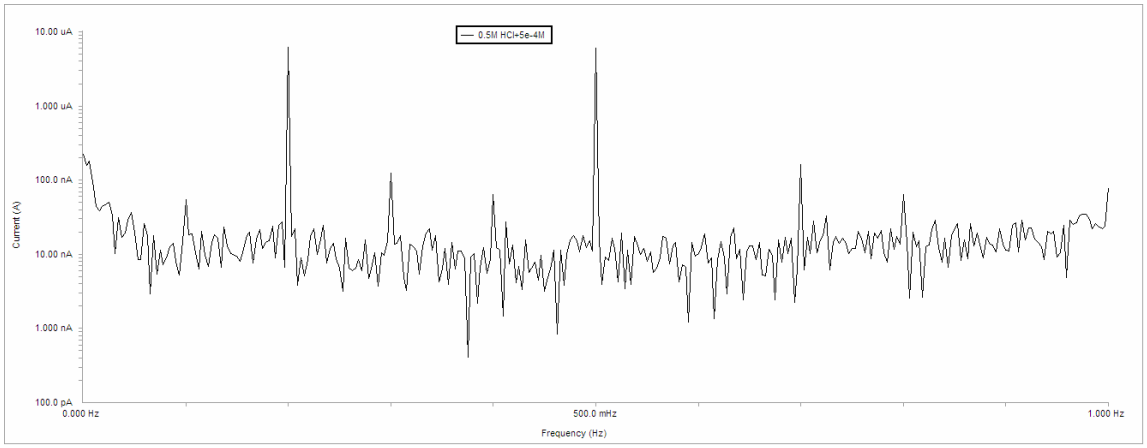

e)

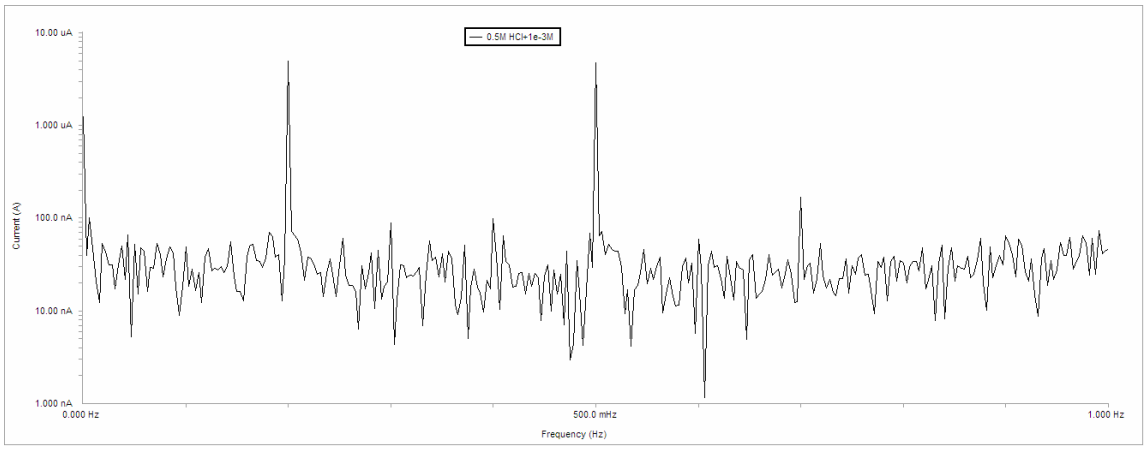

f)

Figures 4a- 4f - Intermodulation spectrum for Al in 0.5 M HCl solutions without and with various concentrations (10^{-5}-10^{-3}M) of compound (I) at 20˚C

The calculated corrosion kinetic parameters at different concentrations of the investigated compounds in 0.5 M HCl at 20 °C (i_{corr}, β_a, β_c, CF-2, CF-3 and % IE) are given in Table 3.

From Table 3, the corrosion current densities decrease by increasing the concentration of investigated compounds and the inhibition efficiencies increase by increasing investigated compounds concentrations. The causality factors in Table 3 are very close to theoretical values which according to EFM theory [48] should guarantee the validity of Tafel slopes and corrosion current densities. Values of causality factors in Table 3 indicate that the measured data are of good quality. The standard values for CF-2 and CF-3 are 2.0 and 3.0, respectively. The deviation of causality factors from their ideal values might due to that the perturbation amplitude was too

small or that the resolution of the frequency spectrum is not high enough also another possible explanation that the inhibitor is not performing very well. The obtained results showed good agreement of corrosion kinetic parameters obtained with the EFM, Tafel extrapolation and EIS methods.

Table 3 - Electrochemical kinetic parameters obtained by EFM technique for aluminum in 0.5M HCl solutions containing various concentrations of the investigated compounds at 20˚C

Concentration, M		i_{corr}, μA cm^{-2}	β_a, mV_{SCE} dec^{-1}	β_c, mV_{SCE} dec^{-1}	Causality Factor (2)	Causality Factor (3)	C.R. mpy	θ	% IE_{EFM}
0.5 M HCl		17.80	91	120	2.13	2.88	38.2	--	--
Compound I	1x10^{-5}	7.97	84	195	1.92	3.13	17.1	0.552	55.2
	5x10^{-5}	6.41	59	166	1.94	2.96	13.8	0.640	64.0
	1x10^{-4}	5.37	53	158	1.85	2.65	11.5	0.698	69.8
	5x10^{-4}	4.65	48	152	1.99	3.14	10.0	0.740	74.0
	1x10^{-3}	2.63	34	136	1.77	3.33	5.6	0.852	85.2
Compound II	1x10^{-5}	8.82	88	160	1.96	3.28	18.9	0.505	50.5
	5x10^{-5}	6.46	53	157	2.15	3.15	13.9	0.637	63.7
	1x10^{-4}	5.63	60	164	1.89	3.24	12.1	0.684	68.4
	5x10^{-4}	4.72	45	147	1. 95	3.06	10.1	0.735	73.5
	1x10^{-3}	2.89	35	137	1.88	2.85	6.2	0.840	84.0
Compound III	1x10^{-5}	8.85	46	149	1.92	3.17	19.0	0.503	50.3
	5x10^{-5}	6.53	71	181	1.87	3.18	14.0	0.633	63.3
	1x10^{-4}	6.27	61	165	1.94	3.05	13.5	0.648	64.8
	5x10^{-4}	4.83	42	143	1.85	2.81	10.4	0.730	73.0
	1x10^{-3}	3.00	48	151	1.87	3.33	6.4	0.832	83.2

From Table 3, the corrosion current densities decrease by increasing the concentration of investigated compounds and the inhibition efficiencies increase by increasing investigated compounds concentrations. The causality factors in Table 3 are very close to theoretical values which according to EFM theory [48] should guarantee the validity of Tafel slopes and corrosion current densities. Values of causality factors in Table 3 indicate that the measured data are of good quality. The standard values for CF-2 and CF-3 are 2.0 and 3.0, respectively. The deviation of causality factors from their ideal values might due to that the perturbation amplitude was too small or that the resolution of the frequency spectrum is not high enough also another possible explanation that the inhibitor is not performing very well. The obtained results showed good agreement of corrosion kinetic parameters obtained with the EFM, Tafel extrapolation and EIS methods.

Figure 5 shows the inhibition efficiencies recorded for the three investigated compounds (I- III) at a concentration of 10^{-4} M using the three different techniques, namely potentiodynamic; EIS and EFM. As seen from this Figure there are good agreement and similar trends. Based on these results, the electrochemical techniques of analysis appear valid for monitoring the corrosion inhibition of aluminum in 0.5 M HCl in the absence and presence of various concentrations of investigated compounds

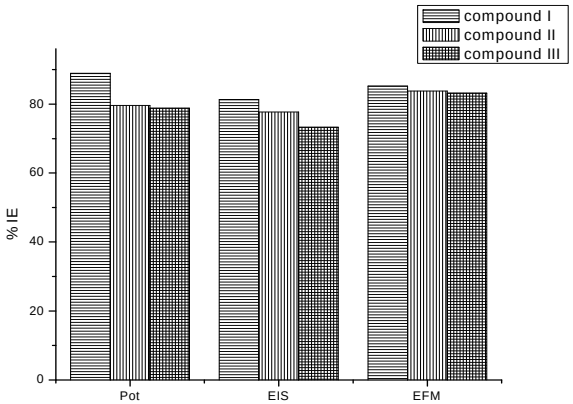

Figure 5 - Comparison of inhibition efficiencies (recorded using potentiodynamic, EIS and EFM measurements) for aluminum in 0.5 M HCl solutions containing 1x10^{-4} M of the investigated Schiff bases at 20˚C

3.4. Adsorption isotherms

It is generally assumed that the adsorption of the inhibitors on the metal surface is the essential step in the inhibition mechanism [49]. To determine the adsorption mode, various isotherms were tested and the Freundlich mode is the best Figure 6, given by Eq.(11) [50]:

$$\theta = K_a C^n \qquad (11)$$

where n is a constant, C is the inhibitor concentration and K_a is the equilibrium constant of adsorption process and is related to the standard free energy of adsorption ΔG°_{ads} by the equation:

$$K_a = 1/55.5 \exp(-\Delta G^\circ_{ads}/RT) \qquad (12)$$

The value of 55.5 is the concentration of water in solution expressed in mole per liter, R is the universal gas constant and T is the absolute temperature. All correlation coefficient (R^2) exceeded 0.99 indicates that the inhibition of Al by these Schiff bases was attributed to adsorption of these compounds on the Al surface. To calculate the surface coverage θ it was assumed that the inhibitor efficiency is due mainly to the blocking effect of the adsorbed species and hence % IE = 100 x θ [51]. The impedance results were used to calculate the adsorption isotherm parameters. The surface coverage θ data are very useful while discussing the adsorption characteristics. The plot of log θ vs.log C for all investigated compounds gave a straight line (Figure 6) characteristic of the Freundlich adsorption isotherm.

The calculated ΔG°_{ads} values, using Eq. (12), were also given in Table 4. $\Delta G^\circ_{ads\ is}$ expressed in kJ mol-1 of Org_{ads}. The negative values of ΔG°_{ads} ensure the spontaneity of the adsorption process and the stability of the adsorbed layer on the Al surface. It is well known that values of ΔG°_{ads} of the order of 40kJ mol^{-1} or higher involve charge sharing or transfer from the inhibitor molecules to metal surface to form coordinate type of bond (chemisorption); those of order of 20 kJ mol^{-1} or lower indicate a physisorption [52- 55].

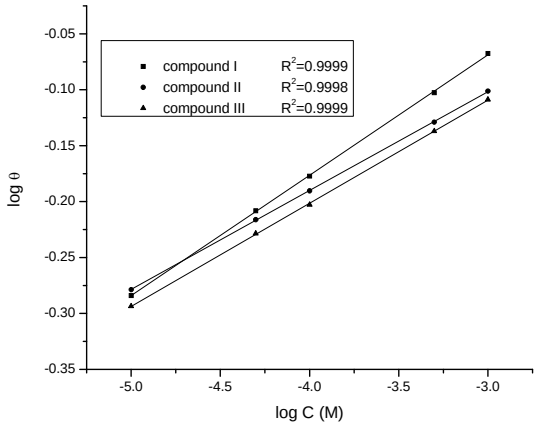

Figure 6 - Curve fitting of corrosion data for aluminum in 0.5M HCl in the presence of different concentrations of surfactant compounds to Freundlich adsorption isotherm at 20°C

The calculated ΔG°_{ads} values (Table 4) are less negative than -20 $kJmol^{-1}$ indicate, therefore, that the adsorption mechanism of the investigated Schiff bases on Al in 0.5 M HCl solution is typical of physisorption. The lower negative values of ΔG°_{ads} indicate that these inhibitors are not strongly adsorbed on the Al surface. Moreover, $|\Delta G^\circ_{ads}|$ of investigated Schiff bases decreases in the order I > II > III. This is in good agreement with the ranking of inhibitors efficiency obtained from the different investigated techniques.

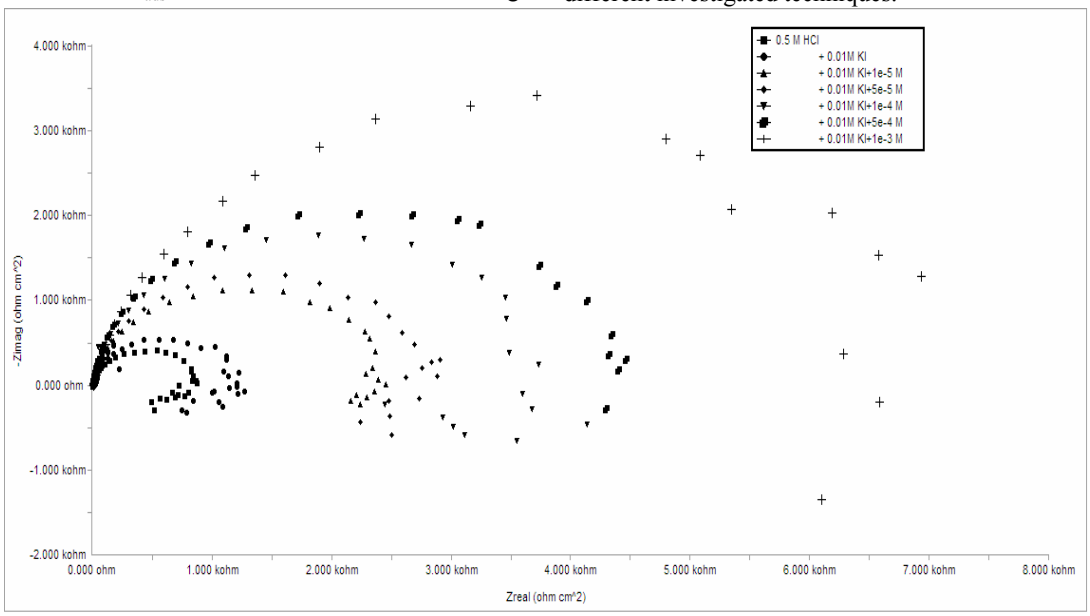

Figure 7a - Nyquist plots recorded for aluminum in 0.5M HCl solutions without and with 10^{-2}M KI various concentrations (10^{-5}-10^{-3}M) compound (I) at the respective corrosion potentials and 20°C

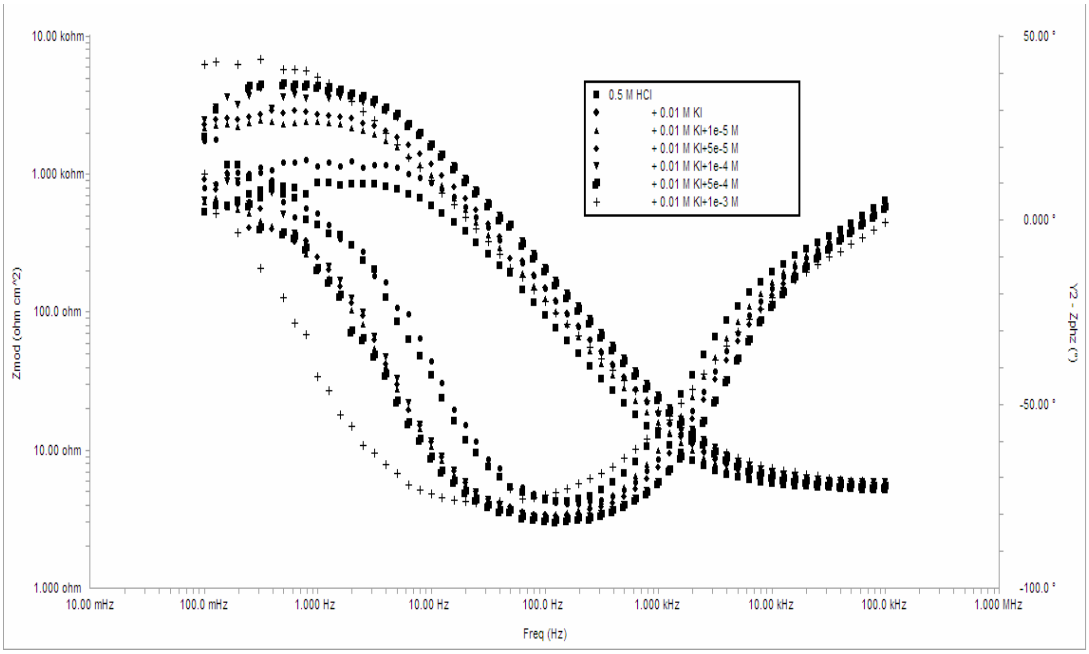

Figure 7b - Bode plots recorded for aluminum in 0.5 M HCl solutions without and with 10^{-2} M KI various concentrations (10^{-5}-10^{-3}M) compound (I) at the respective corrosion potentials and 20˚C

Table 4 - Equilibrium constant and adsorption free energy of the investigated compounds adsorbed on aluminum surface

Inhibitors	Freundlich isotherm		
	n	K	$-\Delta G^{\circ}_{ads.}$, kJ mol^{-1}
Compound I	0.11	1.8	11.4
Compound II	0.09	1.5	11.0
Compound III	0.09	1.4	10.7

Table 5 - Electrochemical kinetic parameters obtained by EIS technique for aluminum in 0.5M HCl solutions in the presence and absence of 10^{-2} M KI and various concentrations of the investigated compounds at 20˚C

		R_{ct}, kΩ cm^2	C_{dl}, μF cm^{-2}	θ	% IE
0.5M HCl		0.71	16.31	--	--
0.5M HCl+0.01M KI		1.030	10.23	0.311	31.1
Compound I	10^{-5}	2.29	12.8	0.691	69.1
	$5x10^{-5}$	2.61	10.5	0.729	72.9
	10^{-4}	3.36	7.43	0.790	79.0
	$5x10^{-4}$	3.82	7.95	0.815	81.5
	10^{-3}	6.30	1.52	0.890	89.0
Compound II	10^{-5}	1.95	18.0	0.637	63.7
	$5x10^{-5}$	2.48	16.4	0.715	71.5
	10^{-4}	3.02	13.1	0.766	76.6
	$5x10^{-4}$	3.48	6.71	0.800	80.0
	10^{-3}	4.60	9.21	0.846	84.6
Compound III	10^{-5}	1.77	15.9	0.601	60.1
	$5x10^{-5}$	2.17	16.7	0.674	67.4
	10^{-4}	2.77	15.9	0.745	74.5
	$5x10^{-4}$	3.02	13.1	0.766	76.6
	10^{-3}	4.48	9.21	0.842	84.2

Table 6 - Electrochemical kinetic parameters obtained by EFM technique for aluminum in 0.5M HCl solutions without and with 10^{-5}M of investigated compounds at different temperatures

Temperature, °C		i_{corr}, μA cm^{-2}	β_a, mV dec^{-1}	β_c, mV dec^{-1}	Causality Factor (2)	Causality Factor (3)	CR, mpy
0.5 M HCl	20	17.80	91	144	2.13	2.88	38.2
	30	19.41	53	133	1.87	3.15	41.7
	40	30.91	52	144	1.75	3.16	66.4
	50	60.86	62	135	1.81	2.84	130.7
	60	94.63	57	125	1.94	2.91	203.2
Compound I	20	5.37	53	138	1.85	2.77	11.5
	30	9.32	59	127	2.04	2.82	20.0
	40	16.18	61	150	1.85	2.82	34.8
	50	30.91	52	144	1.75	3.18	66.4
	60	57.09	59	158	1.69	2.41	122.6
Compound II	20	5.63	60	144	1.89	17.24	12.1
	30	10.33	55	137	1.62	3.46	22.2
	40	18.68	59	148	1.87	3.48	40.1
	50	45.61	60	139	1.87	3.16	98.0
	60	60.86	62	135	1.91	2.84	130.7
Compound III	20	6.27	61	125	1.94	3.05	13.5
	30	12.36	62	138	1.80	2.70	26.5
	40	19. 42	63	146	1.77	3.12	41.7
	50	55.18	52	132	1.62	2.64	118.5
	60	72.94	53	156	1.95	2.95	156.7

3.5. Effect of temperature and activation parameters of inhibition process

The influence of temperature on the corrosion rate of aluminum in 0.5 M HCl in the absence and presence of $1x10^{-4}$ M of the investigated Schiff bases was investigated by the electrochemical frequency modulation technique in temperature range 20 – 60 °C (Table 7).

Table 7 - Activation parameters of the corrosion of aluminum in 0.5M HCl at 10^{-4}M for the investigated compounds

Inhibitors	E_a^*, kJ mol^{-1}	ΔH^*, kJ mol^{-1}	$-\Delta S^*$, J $mol^{-1}K^{-1}$
0.5 M HCl	36.1	14.6	267.8
Compound I	52.0	21.4	236.0
Compound II	50.7	21.0	226.0
Compound III	48.0	19.7	220.9

The dependence of corrosion current density on the temperature can be expressed by Arrhenuis equation:

$$i_{corr} = A \exp(-E^*_a / RT) \quad (13)$$

where A is the pre-exponential factor and E_a^* is the apparent activation energy of the corrosion process. Arrhenuis plot obtained for the corrosion of Al in HCl solution is shown in Figure 8 presents the Arrhenius plot in the presence of $1x10^{-4}$ M investigated Schiff bases. E^*_a values determined from the slopes of these linear plots are shown in Table 8. The linear regression (R^2) is close to 1 which indicates that the corrosion of Al in 0.5 M HCl solution can be elucidated using the kinetic model.

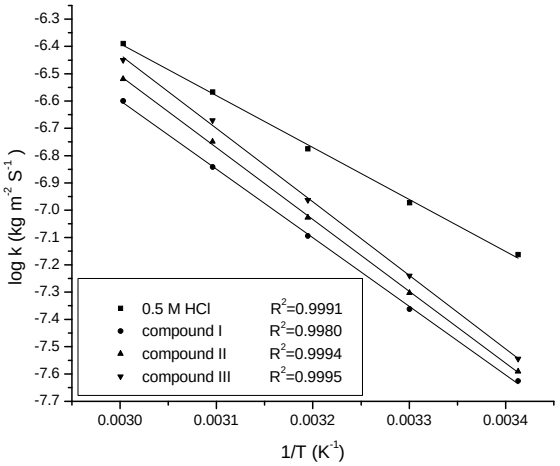

Figure 8 - log k (corrosion rate) – 1/T curves for aluminum dissolution in 0.5M HCl in the absence and presence of 10^{-4} M investigated compounds

Table 8 showed that the value of E^*_a for inhibited solution is higher than that for uninhibited solution, suggesting that dissolution of Al is slow in the presence of inhibitor. It is known from Eq. 13 that the higher E^*_a values lead to the lower corrosion rate. This is due to the formation of a film on the Al surface serving as an energy barrier for the aluminum corrosion [56].

Table 8 - The calculated quantum chemical parameters for investigated compounds

parameter	Compound I	Compound II	Compound III
E_{HOMO} (eV)	-9.000	-9.151	-9.330
E_{LUMO} (eV)	-1.132	-1.218	-1.369
ΔE (eV)	7.868	7.933	7.961
μ (debyes)	2.084	1.378	1.559
η (eV)	3.934	3.967	3.981
σ (eV^{-1})	0.254	0.252	0.251
Pi (eV)	-5.066	-5.185	-5.350
χ (eV)	5.066	5.185	5.350
ΔN (e)	0.795	0.566	0.240

Enthalpy and entropy of activation (ΔH^*, ΔS^*) of the corrosion process were calculated from the transition state theory (Table 7):

$$Rate\ (i_{corr}) = (RT/Nh)\ exp\ (\Delta S^*/R)\ exp\ (-\Delta H^*/RT) \quad (14)$$

where h is Planck's constant and N is Avogadro's number. A plot of log (i_{corr}/ T) vs. 1/ T for Al in 0.5 M HCl at 10^{-4} M investigated compounds, gives straight lines as shown in Figure 9. Values of ΔH^* are positive. This indicates that the corrosion process is an endothermic one. The entropy of activation is large and negative. This implies that the activated complex represents association rather than dissociation step , indicating that a decrease in disorder takes place, going from reactants to the activated complex [57].

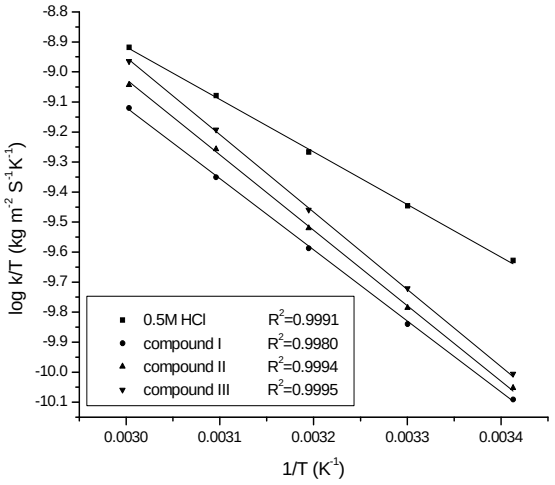

Figure 9 - log k (corrosion rate)/T – 1/T curves for aluminum dissolution in 0.5 M HCl in the absence and presence of 10^{-4} M for of investigated compounds

The order of decreasing inhibition efficiency of the investigated compounds as gathered from the increase in E_a^* and ΔH^* values and decrease in ΔS^* values, is as follows: I > II > III.

3.6. Quantum chemical parameters of investigated compounds

The E_{HOMO} indicates the ability of the molecule to donate electrons to an appropriated acceptor with empty molecular orbitals and E_{LUMO} indicates its ability to accept electrons. The lower the value of E_{LUMO}, the more ability of the molecule is to accept electrons [58].

While, the higher is the value of E_{HOMO} of the inhibitor, the easer is its offering electrons to the unoccupied d-orbital of metal surface and the greater is its inhibition efficiency. The calculations listed in Table 8 showed that the highest energy E_{HOMO} is assigned for the compound I, which is expected to have the highest corrosion inhibition among the investigated compounds. The presence of methoxy group destabilizes the HOMO level which is most observed in the case of compound I Table 8. Therefore, it has the greatest tendency to adsorb on the metal surface and accordingly has the highest inhibition efficiency. This expectation is in a good agreement with the experimental observations suggesting the highest inhibition efficiency for compound I among the other investigated inhibitors Table 8. The compound II has lower E_{HOMO} value than that of compound I which is probably due to the effect of Cl group. So, it is expected that -OCH_3 containing compounds have higher inhibition efficiency than – Cl and -COOH containing compounds. Furthermore, the HOMO level is mostly localized on the two benzene moiety, imino and hydroxyl groups indicating that the preferred sites for electrophilic attack at the metal surface are through the nitrogen and oxygen atoms Figure 10. This means that the two benzene moiety with high coefficients of HOMO density was oriented toward the metal surface and the adsorption is probably occurred through the p-electrons of the two benzene moiety and the lone pair of nitrogen and oxygen. It was found that the variation of the calculated LUMO energies among all investigated inhibitors is rule lessly, and the inhibition efficiency is misrelated to the changes of the E_{LUMO} Table 8.

The HOMO–LUMO energy gap, ΔE approach, which is an important stability index, is applied to develop theoretical models for explaining the structure and conformation barriers in many molecular systems. The smaller is the value of ΔE, the more is the probable inhibition efficiency that the compound has [59-61]. The dipole moment μ, electric field, was used to discuss and rationalize the structure [62]. It was shown from (Table 8) that compound I molecule has the smallest HOMO–LUMO gap compared with the other molecules. Accordingly, it could be expected that compound I molecule has more inclination to adsorb on the metal surface than the other molecules. The higher is the value of μ, the more is the probable inhibition efficiency that

the compound has. The calculations showed that the highest the highest value of μ is assigned for the compound I which has the highest inhibition efficiency. Absolute hardness η and softness σ are important properties to measure the molecular stability and reactivity. A hard molecule has a large energy gap and a soft molecule has a small energy gap. Soft molecules are more reactive than hard ones because they could easily offer electrons to an acceptor. For the simplest transfer of electrons, adsorption could occur at the part of the molecule where σ, which is a local property, has the highest value [63]. In a corrosion system, the inhibitor acts as a Lewis base while the metal acts as a Lewis acid. Bulk metals are soft acids and thus soft base inhibitors are most effective for acidic corrosion of those metals. Accordingly, it is concluded that inhibitor with the highest σ value has the highest inhibition efficiency Table 8 which is in a good agreement with the experimental data.

This is also confirmed from the calculated inhibition efficiencies of molecules as a function of the inhibitor chemical potential, Pi, and the fraction of charge transfer, ΔN to the metal surface. The relatively good agreement of Pi and ΔN with the inhibition efficiency could be related to the fact that any factor causing an increase in chemical potential would enhance the electronic releasing power of inhibitor molecule Table 8.

It was noteworthy that the presence of an electron donating substituent such as -OCH_3 group is more favored than -Cl or -COOH group to increase the inhibition efficiency of the inhibitor. The use of Mulliken population analysis to estimate the adsorption centers of inhibitors has been widely reported and it is mostly used for the calculation of the charge distribution over the whole skeleton of the molecule [64].

There is a general consensus by several authors that the more negatively charged heteroatom is, the more is its ability to adsorb on the metal surface through a donor–acceptor type reaction [65- 67].

Variation in the inhibition efficiency of the inhibitors depends on the presence of electronegative O- and N-atoms as substituents in their molecular structure. The calculated Mulliken charges of selected atoms are presented in Figure 10.

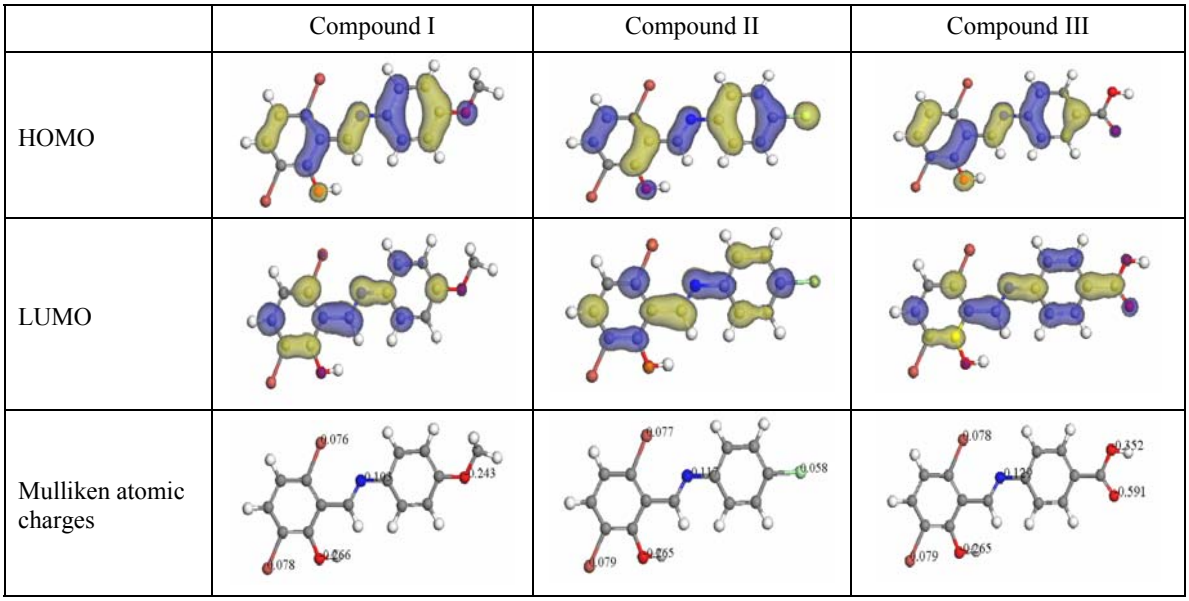

Figure 10 - The optimized molecular structures, HOMO, LUMO and Mulliken atomic charges of the inhibitor molecules using PM3

3.7 Mechanism of Corrosion inhibition

From the observations drawn from the different methods, one can conclude that the inhibitor is adsorbed on Al surface forming a barrier film and protect Al substrate against corrosion in 0.5 M HCl solution. Their inhibitive action can be explained on the basis of the N and O atoms in addition to a π electron interaction of the benzene nucleus with unshared p electrons of Al atoms, which contribute to the donor acceptor bond between the non bonding electron pairs and the vacant orbitals of the metal surface. As far as the inhibition process is concerned, it is generally assumed that adsorption of the inhibitor at the metal/solution interface is the first step in the action mechanism of the inhibitors in aggressive acid media. The adsorption may be the result of one or more of three types of interactions[68, 69], namely; electrostatic attraction between charged molecules and charged metal, coordination of the unshared pairs of electron on the molecule to the metal atom, and involvement of π electrons of the inhibitor molecule in coordination process.

The inhibition efficiency is obviously dependent on the strength of adsorption and this, in term, is affected by the number of adsorption sites and their charge density, molecular size, heat of hydrogenation, mode of interaction with the metal surface and extent of formation of metallic complexes [11]. As, It has been known that, the number of π electrons in the molecule has an important role on the adsorption. It is also, accepted that π electrons of double bonds in a compound can interact with metal surfaces.

It has been found that most of the organic inhibitors act by adsorption on the metal surface [70]. This phenomenon is influenced by the nature and surface charge of metal, by the type of aggressive electrolyte, and by the chemical structure of inhibitors [71].

In general, the investigated Schiff bases may be adsorbed on Al surface in their neutral or protonated forms (cationic form). Since it is well known that the aluminum surface is negatively charged in acid solution [72, 73], so, it is easier for the protonated molecules to approach the negatively charged Al surface due to the electrostatic attraction. In case of adsorption, this involve the displacement of water molecules from the Al surface and sharing electrons between the hetero-atoms and Al. Also, the inhibitor molecules can adsorb on Al surface on the basis of donor-acceptor interactions between π-electrons of aromatic rings and vacant p-orbitals of surface Al atoms. Thus we can conclude that inhibition of Al corrosion in HCl is mainly due to electrostatic interaction. The decrease in inhibition efficiency with rise in temperature (Table 6) supports electrostatic interaction.

5. CONCLUSIONS

1. The investigated Schiff bases are good inhibitors and act as mixed type inhibitors for Al corrosion in HCl solution.

2. The results obtained from all electrochemical measurements show that the inhibiting properties increase with inhibitor concentration. The %IE in accordance to the order: I > II > III with small differences in their numerical values.

3. Double layer capacitances decrease with respect to blank solution when the Schiff base added. This fact may explained by adsorption of Schiff base molecules on the Al surface.

4. The adsorption of Schiff bases on Al surface in HCl solution follows Langmuir adsorption isotherm.

5. The negative values of ΔG°_{ads} show the spontaneity of the adsorption.

6. The values of inhibition efficiencies obtained from the different independent quantitative techniques used showed the validity of the results.

6. REFERENCE

[1] U.Ergun, D.Yuzer and K.C.Emregul, Mater. Chem. Phys., 109(2008)492-499.

[2] T.Hurlen, H.H.Lian, O.S.Odegard and T.V.Valand, Mater.Chem.Phys., 29(1984)579-585

[3] A.K.Maayta, N.A.F.Al-Rawashdeh, Corros.Sci. 46 (2004) 1129.

[4] E.E.Oguzie, Mater.Lett. 59 (2005) 1076.

[5] A. Popova, M. Christov, S. Raicheva, E. Sokolova, Corros. Sci. 46 (2004) 1333.

[6] S.L. Granese, Corrosion 44 (1988) 322.

[7] T. Mimani, S.M. Mayanna, N. Munichandraiah, J. Appl. Electrochem. 23 (1993) 339.

[8] G. Schmitt, K. Bedlur, Werkst. Korros. 36 (1985) 273.

[9] M.A. Hukovic, Z. Grubac, E.S. Lisac, Corrosion 50 (2) (1994) 146.

[10] S.S. Mahmoud, G.A. El-Mahdy, Corrosion 53 (6) (1997) 437.

[11] A.S.Fouda, M.N.Moussa, F.I.Taha and A.I.Elneanaa, Corros.Sci., 26 (1986) 719.

[12] M.N. Desai, B.C. Thakar, P.M. Chiaya, M.H. Gandi, Corros. Sci. 16(1976) 9.

[13] A.Aytac, U.Ozmen and M.Kabbasakaloglu, Mater. Chem.Phys., 89(2005)176.

[14] Y.K.Agrawal, JD Talati, MD Shah, MN Desai, NK Shah, Corros, Sci., 46(2004)633.

[15] K.C. Emregul, O. Atakol, Mater Chem. Phys. 83 (2004)373.

[16] Z. Quan, S. Chen, Y Li, X. Cui, Corros. Sci., 44 (2002)703.

[17] S. Li, Y.G. Wang, S.H. Chen, R. Yu, S. B. Lei, H. Ma, D. Liu, Corros. Sci., 41(1999)1769.

[18] M. Behpour, S. M. Ghoreishi, M. Salavati-Niasari, B. Ebrahimi, Mater Chem. Phys. 107(2008)153.

[19] A. K. Maayta and N. A. F. Rawshdeh, Corros.Sci. 46 (2004) 1129.

[20] M. Stern and A.I.J. Geary, J. Electrochem. Soc., 104 (1957) 56.

[21] R.W. Bosch, J. Hubrecht, W.F. Bogaerts, B.C. Syrett, Corrosion 57 (2001) 60.

[22] S.S. Abdel-Rehim, K.F. Khaled, N.S. Abd-Elshafi, Electrochim. Acta 51 (2006) 3269.

[23] R.G. Parr, D.A. Donnelly, M. Levy, M. Palke, J. Chem. Phys. 68 (1978) 3801.

[24] R. G. Parr, R.G. Pearson, J. Am. Chem. Soc. 105 (1983) 7512.

[25] R.G. Pearson, Inorg. Chem. 27 (1988) 734.

[26] P. Geerlings, F. De Proft, W. Langenaeker, Chem. Rev. 103 (2003) 1793.

[27] V.S. Sastri, J.R. Perumareddi, Corros. Sci. 53 (1997) 617.

[28] I. Lukovits, E. Kalman, F. Zucchi, Corrosion, 57 (2001) 3.

[29] S. Martınez, Mater. Chem. Phys. 77 (2002) 97.

[30] F.Bentiss, C.Jama B.Mernari, H.El Attari, L.El Kadi, M.Lebrini, M.Traisnel and M.Lagrenee, Corros.Sci., 51 (2009)1628.

[31] M.Benabdellah, A.aouniti, A.Dafali, B.Hammouti, M. Benkaddour, A. Yahyi and A.Ettouhami, Appl. Surf. Sci., 252 (2006)8341.

[32] A.A.Aksut, W.J.L.Lorenz and F.Mansfeld, Corros.Sci., 22 (1982) 611.

[33] W.J.Lorenz, and F.Mansfeld, Corros.Sci., 21 (1981) 647.

[34] P.E.Laibinis, and G.M.Whitesides, J.Am.Chem.Soc., 114(1992)9022.

[35] Y.Yamamoto, H.Nishihara and K.Aramaki, J. Electrochem.Soc., 140(1993)436.

[36] R.Haneda and K.Aramaki, J. Electrochem. Soc., 145 (1998)2786.

[37] Y.Feng, W.K.Teo, K.S.Siow, Z.Gao, K.L.Tan and A.K.Hsieh, J.Electrochem.Soc., 144(1997)55.

[38] Z.Quan, X.Wu, S.Chen, S.Zhao and H.Ma , Corrosion, 57(2001)195.

[39] T. Paskossy, J.Electroanal.Chem.364 (1994) 111.

[40] M.Lebrini, M.Lagrenee, H.Vezin, L.Gengembre anf F.Bentiss, Corros.Sci., 47(2005)485.

[41] K.F.Khaled, Electrochim.Acta, 48(2003)2493.

[42] K.Babic-Samardzija, C.Lupu, N.Hackerman, A.R.Barron and A.Luttge, Langmuir, 21(2005)12187.

[43] E.McCafferty and N.Hackerman, J.Electrochem.Soc., 119(1972)146.

[44] J. Bessone, C. Mayer, K. Tuttner, W. J. lorenz, Electrochim. Acta, 28 (1983) 171.

[45] I. Epelboin, M. Keddam, H. Takenouti, J. Appl. Electrochem. 2 (1972) 71.

[46] R.W.Bosch,J.Hubrecht, W.F.Bogaerts and B.C.Syrett, Corrosion,57(2001)60.

[47] F.Bentiss, M.Bouanis, B.Mernari, M.Traisnel, H. Vezin, and .Lagrenee, Appl.Surf.Sci., 253(2007)3696.

[48] R.K.Dinnappa and S.M.Mayanna, J.Appl.Elcreochem. 11 (1982) 111.

[49] A.N.Frumkin, Z.Phys.Chem. 116 (1925) 466

[50] P.W. Atkins, Physical Chemistry, 6th ed., Oxford University Press, 1999, p. 857.

[51] Z. Szlarska-Smialowska, Corros. Sci. 18 (1978) 953.

[52] N. Cahskan, S. Bilgic; Appl. Surf. Sci, 153, (2000), 128.

[53] K. Aramaki, and N. Hackerman; J.Electrochem.Soc., 116, (1969), 568.

[54] L.Tang, X.Li,L.Li,G.Mu,G.Liu,mater.Chem.Phys.97 (2006) 301.

[55] A. S. Fouda, A. A. Al-Sarawy, E. E. El-Katori, Desalination, 201 (2006) 1.

[56] G. Gece, Corros. Sci. 50 (2008) 2981.

[57] D. Q. Zhang, L. W. Gao, G.D. Zhou, Corros. Sci. 46 (2004) 3031.

[58] G. Gao, C. Liang, Electrochim. Acta 52 (2007) 4554.

[59] Y. Feng, S. Chen, Q. Guo, Y. Zhang, G. Liu, J. Electroanal. Chem. 602 (2007)115.

[60] G. Gece, S. Bilgic, Corros. Sci. 51 (2009) 1876.

[61] S. Martınez, Mater. Chem. Phys. 77 (2002) 97.

[62] M. Ozcan, I. Dehri, M. Erbil, Appl. Surf. Sci. 236 (2004) 155.

[63] J.M. Roque, T. Pandiyan, J. Cruz, E. Garcl´a-Ochoa, Corros. Sci. 50 (2008) 614.

[64] F. Kandemirli, S. Sagdinc, Corros. Sci. 49 (2007) 2118.

[65] G. Bereket, C. Ogretic, C. Ozsahim, J. Mol. Struct. (THEOCHEM) 663 (2003) 39.

[66] W. Li, Q. He, C. Pei, B. Hou, Electrochim. Acta 52 (2007) 6386.

[67] S.Rajenran, J.Electrochem.Soc., 54(2)(2005)61.

[68] D.Schweinsberg, G.George, A.Nanayakkara, and D.Steiner, Corros.Sci., 28(1988)33.

[69] S.S.Abd El-Rehim, M.A.Ibrahim amd K.F.Khaled, J.Appl.Electrochem., 29 (1999) 593

[70] J.G.N.Thomas, Some New Fundamental Aspects in Corrosion Inhibitors, Ann.Univ.,Ferrara, N. S. Sez. V. Suppl. N.8. University of Ferrara, Ferrara, Italy, 1981, p. 453.

[71] M.N.Desai, Werkt.U.Korros., 23(1972)475.

[72] A.K.Vijh, J.Phys.Chem., 72(1968)1148.